

**Variable influence of terrain on precipitation patterns:  
Delineation and Use of Effective Terrain Height  
in PRISM**

Christopher Daly  
Director, Spatial Climate Analysis Service  
Oregon State University

July 1998  
Posted to Web: September 2002

An issue encountered when mapping precipitation is the importance of terrain in defining the patterns of precipitation. In the mountainous western U.S., terrain dominates the spatial patterns of precipitation. In flat or gently rolling areas such as the Great Plains, the role of terrain is more subdued, although precipitation variations have been documented over low hills in Illinois (Changnon et al., 1975) and Sweden (Bergeron, 1968), and in narrow valleys in Canada (Longley, 1975). Conceptually, the effectiveness of a terrain feature in amplifying precipitation depends partially on its ability to block and uplift moisture-bearing air. This ability is determined mainly by the profile the feature presents to the oncoming air flow. Steep, bulky features with continuous ridge lines oriented normal to the flow can generally be expected to produce greater precipitation/elevation (P/E) regression slopes than low, gently rising, features with discontinuous ridge lines oriented parallel to the flow. One might imagine a spectrum of “effective” terrain heights, ranging from large features that produce highly three-dimensional (3D) precipitation patterns, to a nearly flat condition which exhibits two-dimensional (2D) patterns only. Between these extremes would be a transition between 2D and 3D patterns, for which P/E slopes would range from zero to values typical of mountainous areas.

Ideally, the effectiveness of the terrain would be reflected in the station data, and thus in the empirical P/E regression slopes. In reality, the station data are rarely of sufficient density and reliability to provide such a detailed and accurate picture. If spatial estimates of the 2D/3D nature of the terrain were available *a priori*, the range of allowable P/E slopes could be varied to the appropriate degree, providing an independent check and constraint (if necessary) on the empirically-derived P/E slopes.

*a. Estimation of effective terrain height*

The effective terrain height for a pixel is estimated by a method similar to that used in estimating the potential wintertime inversion height (Daly et al., in press) . Using a 2.5-min DEM for the U.S., an effective terrain height grid was prepared by: (1) finding the minimum elevation within a approximately 40-km radius of each grid cell; (2) spatially averaging the minimum elevations over a 40-km radius to produce a smooth, “base” elevation grid; (3) subtracting the base elevation grid from the original DEM grid to get an effective terrain height grid; and (4) spatially averaging the effective terrain height grid across a 20-km radius to produce a smooth grid. The effect of moisture-bearing wind direction is not considered in this first

attempt. As discussed in the winter inversion height estimation procedure, sensitivity tests suggested that 40 km was appropriate as the search and averaging radius for discerning significant terrain features. Radii other than 40 km may be appropriate for modeling domains of different size and resolution than the contiguous US at 2.5-min, but we do not yet have enough information to generalize the procedure. The final smoothing at 20 km, which is not done in the wintertime inversion height estimation, was needed to minimize isolated, single-cell terrain discontinuities that do not appear to represent significant blocking features, such as small escarpments in otherwise gently-rolling terrain.

“Significant” terrain features, derived from a first-cut effective terrain height grid for the continental U.S., are shown in Figure 1. As expected, 3D terrain dominates the West and over the Appalachians, with much of central U.S. in 2D territory. In Figure 1, pixels rising at least 100 m above the base terrain field were considered significant 3D features. A firm threshold for effective terrain height that discerns 2D from 3D features has not yet been established, primarily because of limited observational data, weaknesses in our understanding of how small terrain features impact precipitation patterns, and the likelihood that the threshold varies somewhat from region to region.

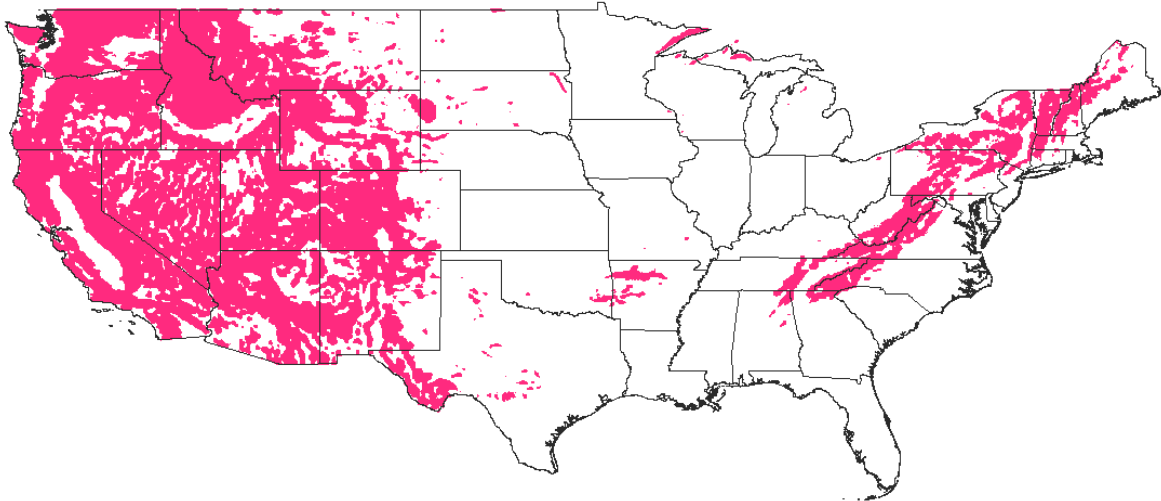


Figure 1. Effective terrain grid for the U.S. Shaded areas denote terrain features that are expected to produce significant terrain-induced (3D) precipitation patterns. Unshaded grid cells as far as 100 km away from the shaded areas may also be considered 3D; see text for discussion. Grid resolution is 2.5 minutes (~ 4 km).

#### *b. Calculation of the effective terrain index*

PRISM uses the effective terrain grid in a multi-step process. A 3D index for the target grid cell ( $I_{3c}$ ) is determined by comparing the effective terrain height of the target cell with

thresholds for 2D and 3D model operation. If the effective terrain height exceeds the 3D threshold,  $I_{3c}$  is set to 1.0. If the effective terrain height is less than the 2D threshold,  $I_{3c}$  is set to 0.0. An effective terrain height between the two thresholds gives a  $I_{3c}$  between zero and one. The calculation is as follows:

$$I_{3c} = \left\{ \begin{array}{l} 1; \quad h_c \geq h_3 \\ \frac{h_c - h_2}{h_3 - h_2}; \quad h_2 < h_c < h_3 \\ 0; \quad h_c \leq h_2 \end{array} \right\} \quad (1)$$

where  $h_c$  is the effective terrain height for the target grid cell, and  $h_2$  and  $h_3$  are user-defined thresholds for 2D and 3D operation, respectively. At the current time,  $h_2$  and  $h_3$  are empirically defined until more robust methods are developed based on a combination of theoretical and observational studies.

If  $I_{3c} < 1$ , signaling a 2D or 2D/3D mixed situation,  $I_{3a}$ , an areal 3D index, is calculated to assess whether the target grid cell is near a significant 3D terrain feature. Precipitation patterns may be affected by the upstream or downstream effects of mountain barriers, well away from the barriers themselves (Smith 1979). Indications of this phenomena have been observed during our analysis of observations in many large valleys in the Western U.S., and it appears to extend approximately 100 km from the nearest 3D terrain features. The 100-km estimate is preliminary, and may be updated as more information is gathered.

$I_{3a}$  is calculated similarly to  $I_{3c}$ :

$$I_{3a} = \left\{ \begin{array}{l} 1; \quad h_a \geq h_3 \\ \frac{h_a - h_2}{h_3 - h_2}; \quad h_2 < h_a < h_3 \\ 0; \quad h_a \leq h_2 \end{array} \right\} \quad (2)$$

where  $h_a$  is a distance-weighted effective terrain height, calculated as

$$h_a = \frac{\sum_{i=1}^n w_i h_i}{n} \quad (3)$$

where  $h_i$  is the effective terrain height for grid cell  $i$  and  $n$  is the number of grid cells within 100 km of the target grid cell. The weight  $w$  for a nearby grid cell  $i$  is

$$w_i = \frac{1}{d_i} \quad (4)$$

where  $d_i$  is the horizontal distance between the centers of the target grid cell and nearby grid cell  $i$ .

The final 3D index,  $I_{3d}$ , is expressed as

$$I_{3d} = \max [I_{3c}, I_{3a}] \quad (5)$$

A scalar from 0 to 1,  $I_{3d}$  represents the degree of importance terrain should play in the estimation of precipitation. When  $I_{3d} = 1$ , the PRISM regression function operates in its normal fashion. As  $I_{3d}$  approaches zero, the influence of terrain is gradually diminished and values of terrain-related parameters -- the minimum, maximum and default regression slopes ( $\beta_{1m}$ ,  $\beta_{1x}$ , and  $\beta_{1d}$ ); and the elevation, facet and layer weighting exponents ( $b$ ,  $c$ , and  $y$ ) -- are reduced to zero (see Daly et al., in press, for details on PRISM parameters):

$$\begin{aligned} \beta_{1mnew} &= I_{3d} \beta_{1m} \\ \beta_{1xnew} &= I_{3d} \beta_{1x} \\ \beta_{1dnew} &= I_{3d} \beta_{1d} \\ b_{new} &= I_{3d} b \\ c_{new} &= I_{3d} c \\ y_{new} &= I_{3d} y \end{aligned} \quad (6)$$

When  $I_{3d}$  is zero, the slope of the precipitation/elevation regression function is forced to zero and stations are weighted by distance and clustering only, resulting in a 2D interpolation.

### c. Calculation of effective terrain weight for a station

If  $I_{3d}$  for the target grid cell less than 1.0, nearby stations in 3D regions must be downweighted in the regression calculations. Consider the example of a large, dry, 2D valley bordered by relatively wet, 3D hills. Including hill stations in precipitation estimates for valley locations would produce a wet bias in the inverse-distance calculations, because elevation is no longer a consideration. Conversely, however, the hill locations can use the valley stations without difficulty in the precipitation-elevation regression function. PRISM handles this situation by assigning an effective terrain weight to each station.

Effective terrain weighting requires that  $I_{3d}$  be calculated for each station. This is done by calculating  $I_{3d}$  for the pixel on which a station resides in exactly the same manner as was described in the previous section for the target grid cell. The effective terrain weight is then

given as

$$V(t) = \begin{cases} 1; & I_{3dc} = 1 \\ \frac{1}{(100|I_{3dc} - I_{3ds}|)^{0.5(1-I_{3dc})}}; & 0 \leq I_{3dc} < 1 \end{cases} \quad (7)$$

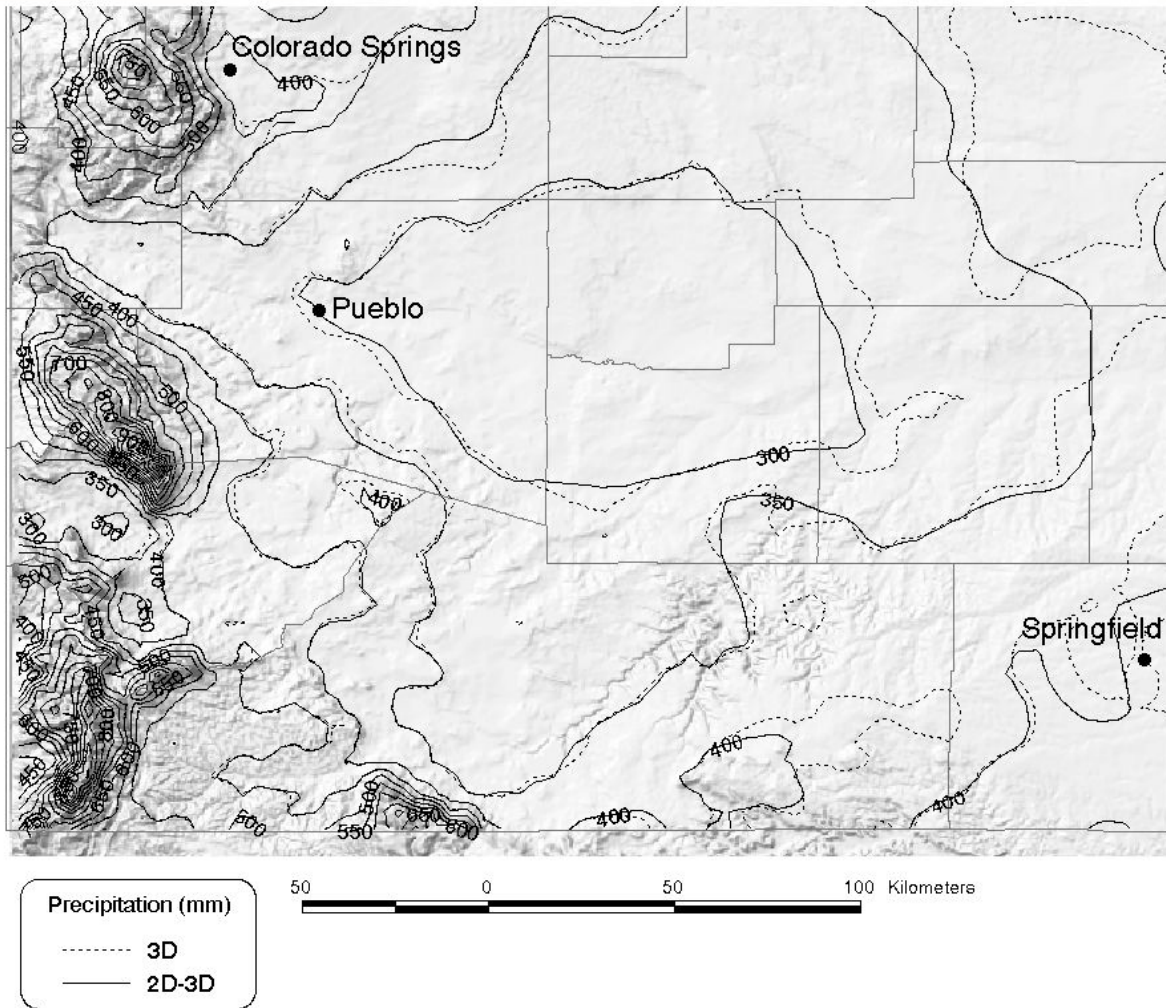
where  $I_{3dc}$  and  $I_{3ds}$  are the effective terrain indices of the target grid cell and station, respectively. When  $I_{3dc}$  is one, indicating the target grid cell is in a 3D situation,  $W(t)$  becomes one and all stations are weighted equally. As  $I_{3dc}$  falls toward zero (a 2D situation), 3D stations are downweighted. The downweighting exponent increases to a maximum of 0.5 as  $I_{3dc}$  approaches zero. When  $I_{3dc} = 0$ , 3D stations are downweighted by a factor of one hundred compared to stations that are in 2D territory.

#### *d. 2D-3D transition zone in southeastern Colorado*

An example of a 2D-3D transition area for precipitation can be found in southeastern Colorado, where the Rocky Mountains (3D) meet the Great Plains (2D). PRISM was run on the region shown in Figure 2 for 1961-90 mean precipitation for each month, and the monthly grids summed to produce a mean annual precipitation map. The dashed contours in Figure 2 show the annual precipitation map as it would appear without use of the effective terrain height grid (3D everywhere). Note the detailed nature of the isohyets over the relatively flat plains area. The solid contours in Figure 2 show the same map, but with the effective terrain grid in use;  $h_2$  was set to 75 m, and  $h_3$  to 250 m. Precipitation contours remain unchanged in the mountainous 3D areas, but are smoother and less detailed in the plains region, reflecting a lack of terrain influence.

#### *e. Conclusions*

An issue encountered when mapping precipitation is the varying importance of terrain in defining the patterns of precipitation. Conceptually, the effectiveness of a terrain feature in amplifying precipitation depends partially on its ability to block and uplift moisture-bearing air flow. To reproduce this concept, a simple grid of effective terrain heights was produced for the U.S. Depending on the height of the effective terrain, PRISM may reduce the influence of terrain information on the precipitation prediction. In flat terrain, PRISM effectively reduces to a cluster, coastal proximity, and distance-weighting algorithm. More sophisticated methods of delineating effective terrain, including barrier orientation to moisture-bearing winds, are planned.



2. PRISM map of 1961-90 mean annual precipitation for eastern Colorado. Dashed contours are without using the effective terrain grid (3D everywhere); and solid contours are using the effective terrain grid (transition from 2D to 3D from plains to mountains). Grid resolution is 2.5 minutes (~ 4 km).

*f. References*

Bergeron, T. 1968. *Studies of the orogenic effect on the areal fine structure of rainfall distribution*. Meteorological Institute, Uppsala Univ., Report No. 6.

Changnon, S. A., Jr., Jones, D. M. A., and Huff, F. A. 1975. Precipitation increases in the low

hills of southern Illinois. Part 2. Field investigation of anomaly. *Monthly Weather Review*, 103: 830-836.

Daly, C., W. P. Gibson, G.H. Taylor, G. L. Johnson, P. Pasteris. 2002. A knowledge-based approach to the statistical mapping of climate. *Climate Research*, 22: 99-113.

Longley, R. W. 1975. Precipitation in valleys. *Weather*, 30: 294-300.

Smith, R. B. 1979. The influence of mountains on the atmosphere. *Adv. Geophys.*, 21: 87-230.